

ECE CORRELATION MEASUREMENTS OF ELECTRON TEMPERATURE FLUCTUATIONS ON TEXTOR USING THE NEW 2-D ECE IMAGING DIAGNOSTIC

I.G.J. Classen¹, M.J. van de Pol¹, S. Leerink¹, A.J.H. Donné¹, C.W. Domier², N.C. Luhmann, Jr.², E. Mazzucato³, T. Munsat³, H.K. Park³, and the TEXTOR team.

¹FOM-Institute for Plasma Physics Rijnhuizen, Association EURATOM-FOM, Partner in the Trilateral Euregio Cluster, PO Box 1207, 3430 BE Nieuwegein, The Netherlands

²University of California at Davis, Dept. of Applied Science, Davis, California, U.S.A.

³Princeton Plasma Physics Laboratory, PO Box 451, Princeton, New Jersey, U.S.A.

e-mail: i.classen@fz-juelich.de

The transport mechanisms in tokamak plasmas are still not fully understood. The experimentally observed high transport levels might be explained by plasma turbulence (electrostatic or magnetic). ECE correlation measurements can give experimental access to plasma turbulence by measuring the fluctuations in the electron temperature.

Recently a new ECE-Imaging (ECEI) system has been installed at TEXTOR. It measures the temperature in a two-dimensional array of sampling volumes. The array is 16 channels vertically by 8 channels horizontally with an inter-channel spacing of about 1 cm. This system will be ideal to study temperature fluctuations by means of correlation measurements.

Introduction

The experimentally determined transport levels in tokamak plasmas are much higher than predicted by neoclassical transport theory. The origin of this so called anomalous transport is thought to be plasma turbulence. Fluctuations of the plasma parameters T_e (electron temperature), n_e (electron density) and electric field E can result in electrostatic drifts resulting in extra radial transport of heat and particles, depending on the phase relations between the fluctuating parameters. Drift waves (Ion/Electron Temperature gradient modes ITG/ETG and Trapped Electron Modes TEM) are theoretically among the most likely instabilities causing the electrostatic fluctuations. As opposed to electrostatic turbulence, also a fluctuating magnetic field can cause extra radial transport.

The newly installed 2-D ECE Imaging (ECEI) diagnostic [1] on TEXTOR ($B_T=1.9-2.6T$, $R=1.75m$, $a=0.46m$) is optimised for measuring small-scale, high frequency temperature fluctuations, giving experimental access to plasma turbulence and the associated anomalous transport. Moreover the system shares optics and sightlines with another fluctuation diagnostic, the new Microwave Imaging Reflectometer (MIR) [2], optimised for measuring density fluctuations. The combined ECEI/MIR system could give information on the phase relation

between temperature and density fluctuations. This paper concentrates on the ECEI system only.

The expected turbulent fluctuation levels are small compared to the (unavoidable) thermal noise in the measured ECE signals. Consequently, a direct observation of temperature fluctuations is not possible. Correlation measurements are necessary to suppress the thermal noise to levels significantly below the expected level of temperature fluctuations. Judging from density fluctuation measurements at TEXTOR [3], the expected fluctuation amplitude is in the order of a few tenths of a percent in the centre, up to a few percent at the edge. The expected frequencies are in the range of 50-100 kHz.

An introduction of the new ECEI system will be given, concentrating on the properties related to correlation measurements. The basics of correlation measurements will be given along with some examples of correlation functions for idealised types of fluctuations. Finally some first results are presented to show that the system is suitable for measuring (radiation) temperature fluctuations with amplitudes much smaller than the thermal noise level. These first results also exemplify some of the difficulties encountered in interpreting correlation measurements. No identification of the measured fluctuations with MHD events or (magnetic or electrostatic) turbulence is attempted.

2-D ECE Imaging system

The newly installed ECEI diagnostic is extensively treated in the EC13 conference contribution by van de Pol [4]. In this paper only the characteristics important for fluctuation measurements are discussed.

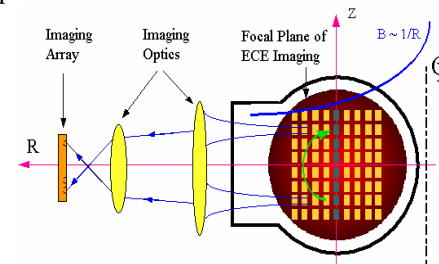


Fig. 1: Schematic overview of the ECEI system

ECEI differs from a conventional ECE radiometer in that the ECE radiation from the plasma is imaged onto an array of 16 detectors (see Fig. 1). This setup enables simultaneous measurement of 16 sightlines. Every sightline is subsequently treated as a normal ECE radiometer with 8 channels. This gives a 2-D array of 8

(horizontally) by 16 (vertically) sample volumes in the poloidal plane, corresponding to an observation area of about 8 by 16 cm in the plasma. The large aperture reflective optics are shared with the MIR system.

The system is designed to observe the second harmonic X-mode ECE radiation in a 4 GHz wide frequency band, tunable over the frequency range of about 100 to 130 GHz. Under normal TEXTOR operation ($B_T=2.25 T$) this gives access to the center and the low field side of the plasma. The inter-channel spacing in radial direction is 0.5 GHz, corresponding to typically 1 cm in the

plasma (on the high field side the inter-channel spacing is smaller than on the low field side due to the 1/R dependence of the toroidal magnetic field).

The inter-channel spacing in vertical direction is determined by the focal plane patterns (the antenna patterns of the array, modified by the optical elements). From the measured focal plane patterns in Fig. 2 a typical inter-channel spacing of 1 cm is found.

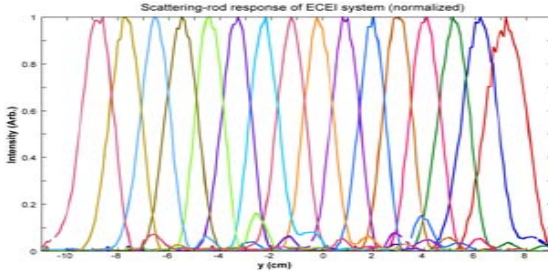


Fig. 2: Focal plane patterns in vertical direction.

The spatial resolution in the direction perpendicular to the line of sight is also determined by the focal plane patterns. The spot sizes in vertical direction (Fig. 2), are typically 12 mm (FWHM) in the focal plane (at the waist of the Gaussian beam patterns). In toroidal direction the spot size is 9 mm. Even and odd channels are separated by 8 mm toroidally due to the zigzagged placement of the antennas on the array, reducing the overlap (cross talk) of neighbouring channels. The focus can be shifted to ensure the observation volume is always in focus.

The spatial resolution in radial direction is determined by the bandwidth of the ECE radiation selected by each channel (the so called IF bandwidth) and by the plasma parameters. The IF bandwidth B_{IF} is set to 300 MHz, corresponding to typically 5 mm in the plasma. This would be the radial resolution if the plasma would emit only one frequency of ECE radiation at every point in space, determined by the local value of the (monotonically decreasing) magnetic field. But the plasma emission is broadened by two important effects; Doppler broadening due to the parallel velocity distribution of the emitting electrons, and relativistic broadening due to the velocity dependence of the electron mass. In observations perpendicular to the magnetic field, as is the case for ECEI, the relativistic broadening is dominant. $T_e \approx 1$ keV gives a broadening of about 1 GHz, corresponding to about 2 cm in the plasma. Luckily, the radiation emitted at the far side of this broadened emission profile is mostly absorbed before it reaches the observer. For typical TEXTOR parameters the width of the visible layer of plasma is always below 5 mm. This width determines, along with the IF bandwidth of the ECE system, the radial resolution. Adding the 5 mm resulting from the finite IF bandwidth gives a radial resolution below 1 cm.

The time resolution is determined by the so-called video bandwidth B_V of the system. The maximum B_V , and hence the maximum detectable fluctuation frequency, is currently set to 240 kHz (sampling frequency 500 kHz $\approx 2B_V$).

Increasing B_V (better time resolution) or decreasing B_{IF} (better spatial resolution) increases the thermal noise level according to [5]:

$$\frac{\sqrt{\langle \Delta T_R^2 \rangle}}{\langle T_R \rangle} = \sqrt{\frac{2B_V}{B_{IF}}} \quad \text{Eq. 1}$$

Taking $B_{IF}=300$ MHz and $B_V=240$ kHz gives a thermal noise level of 4%. This value is close to the experimentally observed noise levels of the ECEI system.

Optical thickness

The optical thickness is a very important plasma parameter for the interpretation of fluctuation measurements. For 2nd harmonic X-mode radiation well below cut-off the optical thickness τ_0^{2X} is [6]:

$$\tau_0^{2X} = \frac{\pi k_B e}{\epsilon_0 m_e c^3} \cdot n_e T_e \cdot \frac{R^2}{B_0 R_0} \quad \text{Eq. 2}$$

Only in optically thick plasmas ($\tau \gg 1$) the measured radiation intensity reaches the Rayleigh-Jeans intensity, and is consequently only a function of electron temperature. In optically thin plasmas, the measured radiation temperature T_R can be expressed as:

$$T_R = T_e (1 - e^{-\tau}) \quad \text{Eq. 3}$$

where the optical thickness τ is a function of both n_e and T_e . So not only temperature fluctuations, but also density fluctuations will result in fluctuations of T_R . A first order approximation gives [6]:

$$\frac{\tilde{T}_R}{\langle T_R \rangle} = (1 + a) \frac{\tilde{T}_e}{\langle T_e \rangle} + a \frac{\tilde{n}_e}{\langle n_e \rangle} \quad \text{with} \quad a = \frac{\tau \cdot \exp(-\tau)}{1 - \exp(-\tau)} \quad \text{Eq. 4}$$

For example for $\tau=2$ about 30% of the density fluctuation level is seen in T_R . Only for $\tau > 6$ density fluctuations hardly influence T_R . So one should be very careful in interpreting fluctuations measured with ECE as electron temperature fluctuations.

Noise reduction: Correlation

The thermal noise can be suppressed by cross correlating two signals with independent noise [6]. The fluctuations that are present in both signals will survive the cross correlation and will be revealed in the cross correlation function. The cross correlation function $C_{12}(l)$ of two signals $S_1(t)$ and $S_2(t)$, as a function of the time lag l can be written as

$$C_{12}(l) = \lim_{T_M \rightarrow \infty} \frac{1}{T_M} \int_0^{T_M} S_1(t) S_2(t+l) dt \quad \text{Eq. 5}$$

where T_M is the time over which S_1 and S_2 are measured. $C_{12}(l)$ can be seen as the dot product between S_1 and S_2 shifted by a time lag l . If $S_1=S_2$ one speaks of the

auto correlation function. Figure 3 gives some examples of correlation functions for some idealised synthetic signals. The amplitude of the (correlated part of the) fluctuations is found by taking the square root of the amplitude in C_{12} .

Correlating (discrete) signals of length N reduces the noise by a factor of $N^{1/2}$. Because fluctuations are contained quadratically in C_{12} , this leads to a minimal detectable fluctuation level of

$$\frac{\sqrt{\langle \tilde{T}_R^2(t) \rangle}}{\langle T_R(t) \rangle} = N^{-1/4} \sqrt{\frac{B_V}{B_{IF}}} \quad \text{Eq. 6}$$

For ECEI at maximal sampling rate, taking 2s of data (10^6 data points), this theoretically leads to a minimal detectable fluctuation level of about 0.1 %.

Correlated broadband phenomena with bandwidth B (of which thermal noise in an autocorrelation is an example with bandwidth B_V) cause a peak in C_{12} that falls off with a decay time

$$\tau_{1/2} = \sqrt{\frac{\ln 2}{\pi}} \cdot \frac{1}{B} \quad \text{Eq. 7}$$

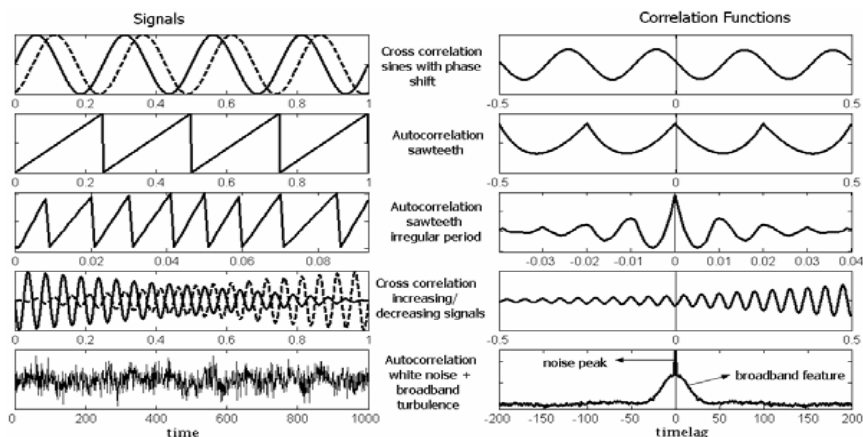


Fig 3: Examples of correlation functions for typical signals.

First results

First measurements of broadband fluctuations with ECEI are shown in figure 4. The data was taken around normalized plasma radius $\rho=0.75$ at the low field side during an Ohmic plasma (shotnumber 94555) with $B_T=2.55$ T, $I_p=350$ kA and a central density of $2.3 \cdot 10^{19} \text{ m}^{-3}$. One second of 200 kHz data was used for building the correlation functions. A high pass filter is applied on the correlation functions to get rid of 50 Hz oscillations present in the data.

As seen from the autocorrelation the broadband feature has a relative amplitude of 0.5 % and a bandwidth of about 10 kHz (eq. 7). Figure 4 also shows the cross correlation functions for a number of poloidal and radial channel separations. From the decay of the peak height an estimate of the correlation lengths can be made. In poloidal direction a clear decay is seen, leading to a correlation length in the order of 3cm. In radial direction no strong decay is observed over 5 cm. The peaks in the cross correlation functions do not show a significant displacement in timelag from which a velocity could be derived. So either the velocity is too fast to detect (faster than about 10 km/s) or zero.

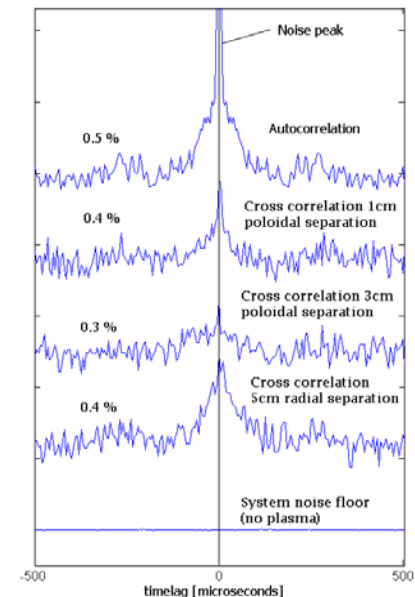


Fig. 4: Broadband fluctuation measurement (for clarity the signals are offset)

Finally figure 4 shows the correlation function of data taken without plasma. No features are visible, showing that the broadband peak is not an artifact of the system noise of the ECEI system.

The optical thickness for the data shown was about 1, so whether the fluctuations are temperature or density fluctuations can not be determined without information from other diagnostics like the MIR reflectometer.

Conclusions and outlook

The new TEXTOR 2-D ECEI diagnostic is suitable for the correlation measurement of small-scale, high frequency fluctuations. Spatial and temporal resolutions are sufficient and the theoretical noise reduction is observed, leading to a fluctuation sensitivity of about 0.1%. Although the interpretation of correlation measurements is difficult due to the necessary long integration times, they could give insight into turbulent transport.

References

- [1] H. Park et al., *Review of Scientific Instruments* **74**, 4239-4262 (2004).
- [2] E. Mazzucato, *Nuclear Fusion*, 2001,**41**,203
- [3] A. Krämer-Flecken, *EPS2003, ECA Vol 27A*, P-2.135
- [4] M.J. van de Pol, "2-D ECE Imaging experiments at TEXTOR", This Conference
- [5] G. Bekefi, "Radiation processes in Plasmas", New York, Wiley 1996.
- [6] S. Sattler, PhD thesis Max-Planck-Institut für Plasmaphysic, IPP III/193, 1993

This work, supported by the European Communities under the contract of the Association EURATOM/FOM, was carried out within the framework of the European Fusion Programme with financial support from NWO. The views and opinions expressed herein do not necessarily reflect those of the European Commission.

This work is supported by the U.S. Department of Energy under contracts No. DE-FG03-95ER54295, DE-FG03-99ER54531 and DE-AC02-76-CHO-307.